SkinSource: A Data-Driven Toolbox for Predicting Touch-Elicited Vibrations in the Upper Limb

Neeli Tummala[1,*], Gregory Reardon[2,*], Simone Fani[5], Dustin Goetz[3], Matteo Bianchi[6], and Yon Visell[1,2,3,4]

***Abstract*— Vibrations transmitted throughout the hand and arm during touch contact play a central role in haptic science and engineering but are challenging to model or experimentally characterize. Here, we present SkinSource, a data-driven toolbox for predicting skin vibrations across the upper limb in response to user-specified input forces. The toolbox leverages impulse response measurements that encode the physics of vibration transmission across the hands and arms of four participants and provides software tools for analyzing the predicted skin responses. We show that the SkinSource predictions closely match experimental measurements and confirm the underlying assumption of linear vibration transmission in the skin. We also demonstrate through several usage examples how SkinSource can act as a versatile computational platform for haptic research applications, such as characterizing vibrotactile transmission in the skin, engineering haptic interfaces, and investigating touch perception.**

I. Introduction

Manual touch interactions and haptic feedback supplied to the hand generate vibrations that are transmitted throughout the hand and arm [1], [2]. These evoked vibrations encode perceptually relevant information about the contact events that elicit them [3]–[5]. Characterizing this mechanical process has played an important role in understanding the interplay between biomechanics and neural encoding in touch perception [6]–[13]. Investigations of vibration transmission in the upper limb have also informed the engineering of vibrotactile feedback techniques [14], [15] and inspired new approaches for engineering robotic or prosthetic sensing systems [16]–[18]. Moreover, touch-elicited skin vibrations have been leveraged in the design of wearable sensing and haptic feedback devices [19]–[23]. Outside of haptic technology, vibration transmission in the upper limb has been characterized to inform the development of occupational safety standards for power tool usage [24] and diagnostic tests for skin diseases [25].

However, vibration transmission in the upper limb is a complex function of the anatomical structure and tissue biomechanics of the hand and arm [8], [14], [26]–[28]. It has thus proven challenging to accurately predict the whole-limb response from numerical modeling. Such models have been most effective at characterizing the mechanical response of localized tissues near the stimulation site [26], [29] or capturing the dynamics of the musculoskeletal system [30] rather than predicting vibration transmission across the entire limb. Further, due to the widespread transmission of touch-elicited vibrations throughout the hand and arm [1], [2], experimental measurements require time-consuming procedures and specialized equipment [5], [8], [14], [25]. As a result, measurements are often limited in scope, employing a single stimulation location and application-specific test signals.

Here, we introduce SkinSource, a data-driven, open-source toolbox for accurately predicting skin vibrations across the upper limb in response to input forces applied at any of 20 distinct locations on the hand. The toolbox integrates a vibrometry dataset containing impulse response measurements captured at 72 locations on the hands and arms of four participants and exploits the linearity of vibration transmission in the skin to predict the mechanical response of the upper limb. SkinSource also includes MATLAB tools that enable users to design their own stimuli to apply at one or more hand locations and analyze the predicted skin vibrations in the time or frequency domains.

The functionalities provided by SkinSource are intended to aid haptics research, engineering, and design, like other recently released haptics datasets and tools [9], [31]. SkinSource can serve researchers in sensory neuroscience and perception by providing a means for investigating the mechanical basis of touch perception. The toolbox may also aid engineers in designing haptic interfaces, wearable sensors, or assistive devices while reducing the need for laboratory experiments (Fig. 1A). In the remainder of the paper, we provide an overview of the toolbox and potential use cases (Section II), describe the data collection (Section III), report results validating the toolbox predictions (Section IV), and confirm the linearity of vibration transmission in the upper limb (Section V).

II. The SkinSource Toolbox

SkinSource contains a vibrometry dataset (Sec. IIA) and accompanying MATLAB software tools that allow users to specify time-varying force inputs at any of 20 locations on the hand. Skin vibrations are predicted at 72 locations on four upper limb models via convolution with impulse responses measured from four participants (Sec. IIB). These predictions are returned to users as an array of 3-axis skin accelerations. SkinSource also provides data exploration tools that allow

*N.T. and G.R. contributed equally

[1]N.T. and Y.V. are with the Department of Electrical and Computer Engineering, [2]G.R. and Y.V. are with the Media Arts and Technology Program, [3]D.G. and Y.V. are with the Department of Mechanical Engineering, and [4]Y.V. is with the Department of Biological Engineering, University of California, Santa Barbara, Santa Barbara, CA 93106, USA yonvisell@ucsb.edu

[5]S.F. is with the School of Biological and Health Systems Engineering, Arizona State University, Tempe, AZ 85281, USA, and the Soft Robotics for Human Cooperation and Rehabilitation Lab, Instituto Italiano di Tecnologia, Geneva, GE 16163, Italy

[6]M.B. is with the Department of Information Engineering, University of Pisa, PI 56122, Italy

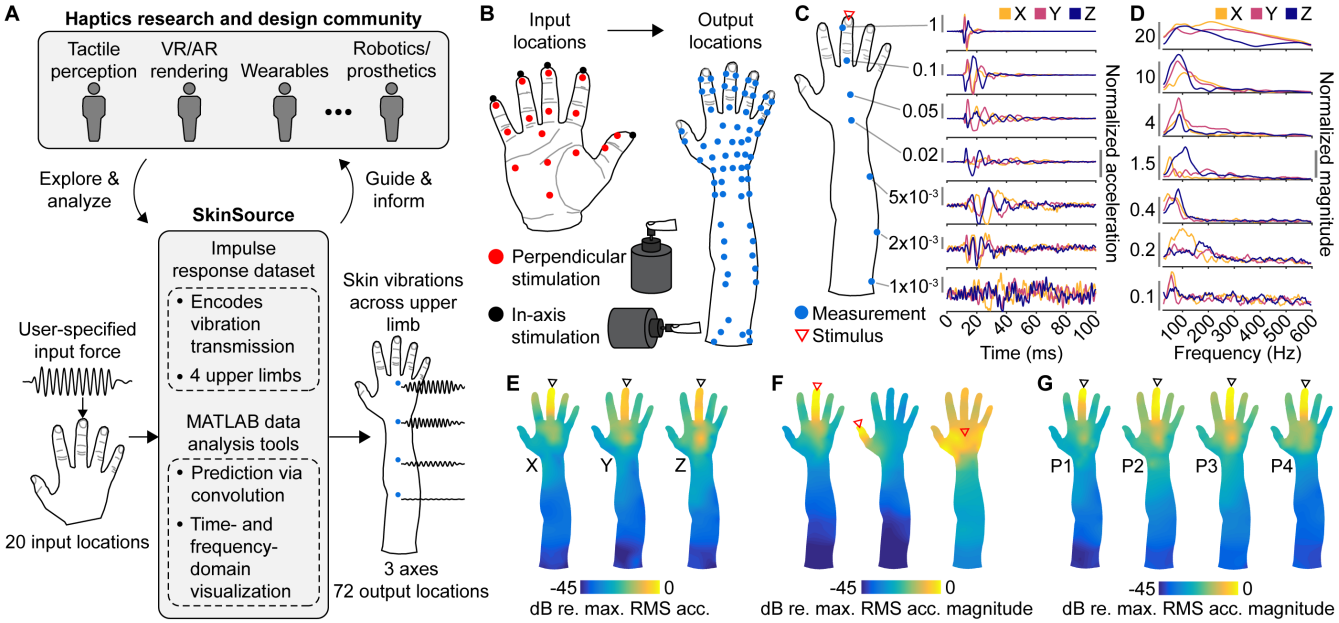

Fig. 1. **Overview of SkinSource and impulse response dataset.** A) Users in the haptics community can utilize SkinSource to explore and analyze vibration transmission in the upper limb and use the outputs to guide and inform research and design applications. B) Force inputs can be supplied at any of 20 locations on the palmar surface of the hand (left) perpendicular to the hand surface (red dots) or in-axis with the digits (black dots). Skin vibrations (accelerations) are predicted at 66 locations on the dorsal surface (and 6 locations on the volar surface, not pictured) of the upper limb (right). C) Normalized 3-axis impulse responses at selected output locations (blue dots) on the upper limb of Participant 4 (P4) for an input applied at the tip of digit III (perpendicular). D) Normalized 3-axis frequency magnitude spectrums of the impulse responses shown in C. E) Normalized RMS of 3-axis impulse responses across each measurement axis for an input at the tip of digit III (in-axis) of P3. F) Normalized RMS of impulse response acceleration magnitudes for inputs applied at 3 locations (red arrows, all perpendicular) on the hand of P1. G) Normalized RMS of impulse response acceleration magnitudes for an input at the tip of digit III (perpendicular) on the hands of all participants.

users to project vibrations onto selected axes, compute frequency-domain spectra, and visualize vibrations on a 2D upper limb model. The results shown in Fig. 1 and Fig. 2 were generated using SkinSource and demonstrate the versatility of the toolbox for applications in characterizing the mechanical response of the upper limb, designing haptic devices, and investigating touch perception. SkinSource can be found at `https://doi.org/10.5281/zenodo.10547601` along with documentation and usage examples.

A. Impulse Response Dataset

SkinSource integrates a dataset of more than 5000 impulse responses obtained from 3-axis vibrometry measurements of skin acceleration on the upper limbs of four participants (sample rate: 1300 Hz), as described in detail in Section III. The impulse responses encode the physics of vibration transmission from 20 input locations on the palmar surface of the hand to 72 output locations on the hand and arm (66 dorsal, 6 volar; Fig. 1B). The measured impulse responses capture previously reported features of vibration transmission in the skin. These features include frequency-dependent transmission speed (phase velocity) [8], demonstrated by the temporal spreading of a wave packet with increasing transmission distance (Fig. 1C), and frequency-dependent attenuation, with lower frequency vibrations generally exhibiting less attenuation [14] (Fig. 1D). Moreover, the impulse responses demonstrate that measurable mechanical energy is transmitted to the wrist and forearm, also reflecting findings from prior work [1], [3], [23]. The dataset enables investigations of skin vibrations measured in different axes (Fig. 1E) and analyses of vibration transmission for different input locations (Fig. 1F). Additionally, the dataset allows users to investigate the differences in vibration transmission across different upper limbs by providing data collected from four participants (Fig. 1G; see Section III).

B. Toolbox Implementation

To predict skin vibrations in the upper limb elicited by a user-specified input stimulus, SkinSource leverages the measured impulse response dataset. This implementation relies on the assumption that vibration transmission in the skin is approximately linear for some small signal regime and can therefore be described compactly as impulse responses or, equivalently, as frequency domain transfer functions. This assumption of linearity is validated and discussed in Section V. In this linear regime, vibrations elicited by arbitrary time-varying forces $f_{\mathbf{y}_n}(t)$ applied normal to the skin at location $\mathbf{y}_n$ can be efficiently computed as

$$u^{\alpha}(\mathbf{x},t) = \sum_{n=1}^{N} h^{\alpha}_{\mathbf{y}_n}(\mathbf{x},t) * f_{\mathbf{y}_n}(t), \tag{1}$$

where $*$ is convolution in time, N is the number of input locations, $u^{\alpha}(\mathbf{x},t)$ is the time-varying skin vibration in direction α at location $\mathbf{x}$, and $h^{\alpha}_{\mathbf{y}_n}(\mathbf{x},t)$ is the time-varying skin vibration in direction α at location $\mathbf{x}$ elicited by a unit impulsive force applied normal to the skin at location $\mathbf{y}_n$ (the impulse response). Measuring the impulse responses

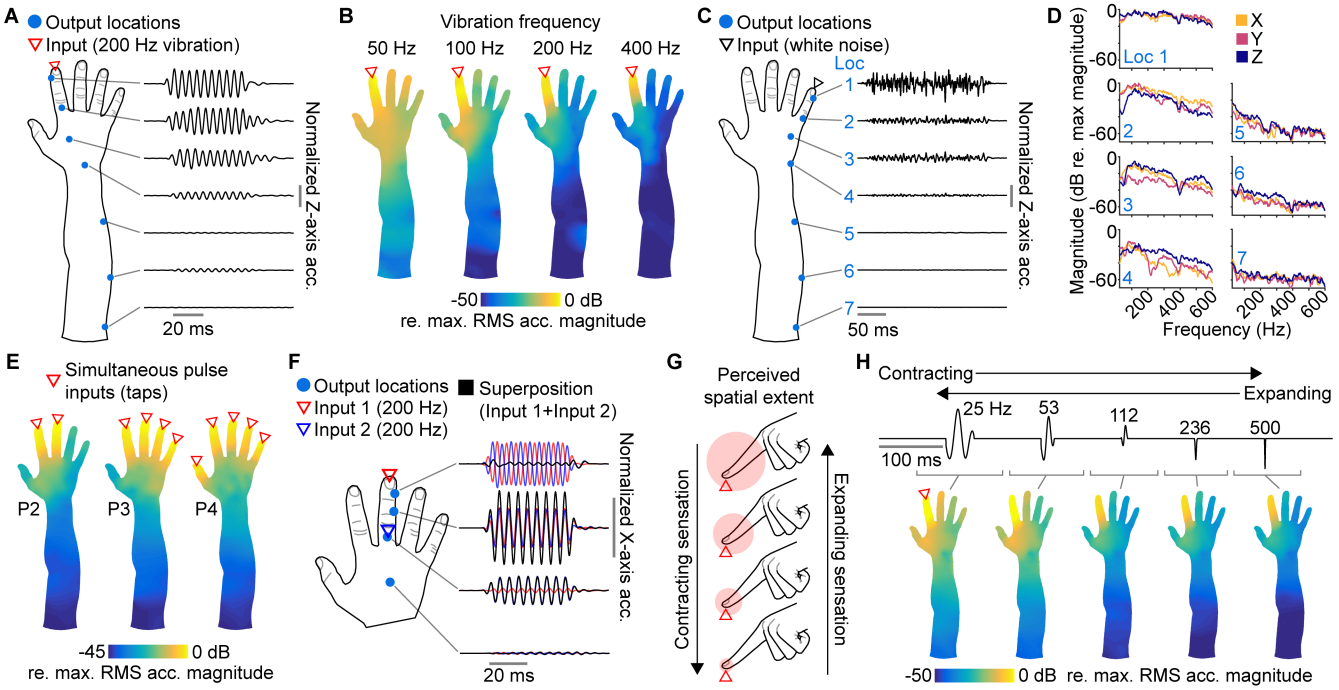

Fig. 2. **SkinSource usage examples.** A) Normalized z-axis skin acceleration at selected locations (blue dots) on the upper limb of Participant 1 (P1) elicited by a 200 Hz sinusoidal vibration applied at the tip of digit II (perpendicular). B) Normalized RMS of skin acceleration magnitudes for 4 input sinusoids of varying frequencies (50, 100, 200, 400 Hz) applied to the tip of digit II (perpendicular) of P1. C) Normalized z-axis skin acceleration at selected locations (blue dots) on the upper limb of P2 elicited by a white noise stimulus applied at the tip of digit V (in-axis). D) Normalized 3-axis frequency spectrum magnitudes of skin accelerations shown in C. E) Normalized RMS of skin acceleration magnitudes elicited by the simultaneous application of pulses at the locations marked by red arrows (perpendicular) across three different participants (P2, P3, and P4). F) Normalized x-axis skin acceleration at selected locations (blue dots) on the hand of P3 elicited by a 200 Hz vibration applied at the tip of digit III (red, perpendicular), a 200 Hz vibration applied at the base of digit III (blue, perpendicular), and the superposition of both input vibrations (black). G) Perceived spatial extent of vibrations provided to the tip of digit II in a haptic illusion created by [14] that elicits a spatially contracting (top to bottom) or expanding (bottom to top) sensation using a single actuator. H) Normalized RMS of skin acceleration magnitudes within 5 consecutive time windows elicited by the stimulus that produces the illusion in G, which is a train of wavelets varying in frequency (top, black trace) applied at the tip of digit II (perpendicular) of P4.

eliminates the need for multiple experimental measurements of skin vibrations elicited by different input stimuli of interest. Instead, resulting vibration responses can be predicted efficiently *in silico* (< 100 ms computation time).

SkinSource provides four different data-driven models built on measurements obtained on the upper limbs of four different participants. Although anatomical features and therefore distances between accelerometers varied across participants (hand lengths: 165 to 185 mm), input and output locations were mapped to a single 2D dorsal hand surface for visualization and analysis purposes. Measured skin vibrations were extrapolated to points on the boundary of the 2D hand surface using weights proportional to the distance of the two accelerometers closest to each boundary point. Skin vibrations at intermediate locations on the 2D hand surface were then determined using natural neighbor interpolation. SkinSource also integrates a number of MATLAB software tools to aid users in analyzing the predicted skin vibrations, including projecting the 3-axis vibrations onto specified axes (e.g., the tangential or principle component axis) and computing frequency domain spectra.

C. Toolbox Usage and Examples

In this section, we briefly explore several potential applications of SkinSource.

1) Designing Haptic Devices: SkinSource can facilitate the haptic device design process by predicting skin vibrations elicited by mechanical stimuli. For example, users can input sinusoidal vibrations of various frequencies to the hand (Fig. 2A) and analyze properties of vibration transmission in the upper limb, such as frequency-dependent attenuation (Fig. 2B). Such observations of vibration transmission have led to the establishment of device guidelines like the optimal configuration of vibrotactile stimulators in haptic feedback displays [32], [33] and to the engineering of haptic sensing devices that leverage touch-elicited vibrations [19]–[23].

2) Understanding Tactile Perception: Prior studies of vibration transmission in the skin have demonstrated that texture-elicited vibrations play a role in human tactile perception [1], [4]. To aid in such investigations in the future, SkinSource can be used to examine skin vibrations elicited during texture exploration. For example, users can predict the skin vibrations elicited by a texture approximated as white Gaussian noise during transmission across the entire upper limb in both the time (Fig. 2C) and frequency domains (Fig. 2D). SkinSource can also be easily integrated with texture datasets captured during scanning of the fingerpad [4], [34].

3) Investigating Complex Manual Interactions: Many manual touch interactions, such as grasping a cup or typing on a keyboard, involve multiple points of touch contact on

the hand. With SkinSource, users can investigate vibrations elicited by interactions that can be approximated as the superposition of force inputs at multiple hand locations. For example, pulse inputs applied simultaneously at several fingertips (Fig. 2E) closely resemble whole-hand vibrometry measurements collected during multi-finger tapping gestures [2]. Moreover, the exploration of superimposed inputs can produce interesting results, such as constructive and destructive interference at various regions on the skin after the application of simultaneous vibrations at multiple locations (Fig. 2F, top trace: destructive, second-to-top trace: constructive). Similar investigations enabled by SkinSource could be used to engineer multi-input stimuli for focusing vibrations in the skin [15] or to optimize actuator locations in virtual reality gloves [35].

4) Engineering Tactile Feedback Techniques: Examining vibration transmission in the skin can guide the creation of new tactile feedback techniques. This process is clearly exemplified in [14], where the authors observed frequency-dependent attenuation of skin vibrations in their mechanical measurements and used this observation to engineer a novel perceptual effect of spatial expansion or contraction using only a single actuator (Fig. 2G). This iterative design process could be accelerated with SkinSource, which allows users to rapidly explore skin vibrations elicited by different test signals. For example, users can observe frequency-dependent attenuation in the skin by inputting sinusoidal vibrations (Fig. 2B). They can then design and test novel vibrotactile stimuli exploiting this phenomenon, such as the expanding/contracting stimulus designed in [14]. The spatial extent of the skin vibrations predicted by SkinSource in response to this stimulus do, in fact, contract and expand (Fig. 2H), indicating a promising perceptual effect for users to later test. The iterative design process described in this section can also be employed for many other applications, including the design of wearable and robotic sensing technology.

III. Impulse Response Dataset Capture

A. Experimental Setup

Skin accelerations were measured using custom accelerometer arrays [2] placed on the right hands and arms of four participants (two female, two male, ages in years: mean 27.5 $\pm$ 3.1 SD; Fig. 3A). The experimental protocol was approved by the Human Subjects Committee at UC Santa Barbara and complied with the Declaration of Helsinki. All participants gave their written and informed consent. Each of the 72 accelerometers in the array was adhered to the skin using double-sided adhesive (66 on the dorsal surface, 6 on the volar surface). Though hand sizes differed (165 to $185\,\mathrm{mm}$), the relative anatomical positioning of each accelerometer was preserved across participants. The stimuli were applied with an electromagnetic actuator (Mini Shaker Type 4810, Brüel & Kjær, Denmark) at 20 input locations on the volar surface of the hand either perpendicular to the volar hand surface (Fig. 3B) or in-axis with the digits (Fig. 3C). The actuator probe tip (square profile, $49\,\mathrm{mm}^2$ contact area) was attached to the skin with double-sided adhesive to ensure that

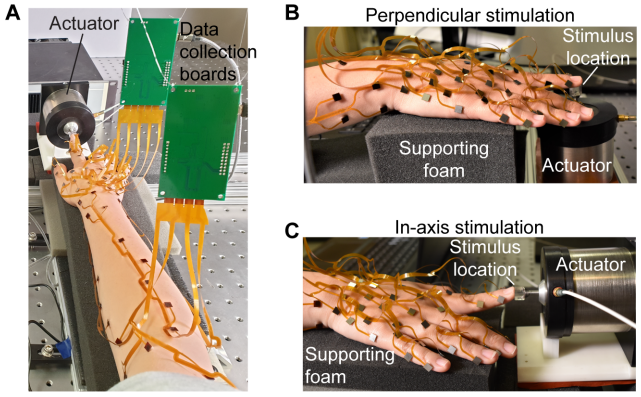

Fig. 3. **Impulse response dataset capture.** A) Data was captured using an accelerometer array on the upper limb, which was supported by foam but otherwise unconstrained. Stimuli were delivered both B) perpendicular to the palmar surface of the hand and C) in-axis with the digits.

there was no decoupling during the application of the stimuli. Each participant was seated with their hand and forearm placed palm-down in a comfortable resting position on a pneumatically-isolated table. The volar side of the hand and forearm were supported by foam in all areas except where the stimulus was applied. The upper limb was otherwise unconstrained. Participants were instructed to keep their hands relaxed throughout the experiment without applying force to the probe tip beyond that applied through their resting posture. Thus, the actuator preload was minimal, and the probe tip was primarily secured in place via the double-sided adhesive.

B. Data Collection and Processing

Skin accelerations were collected in 3 axes at a sample rate of $1300\,\mathrm{Hz}$. The z-axis was normal to the skin surface, while the x- and y-axes were tangential to the skin surface. However, the x- and y-axes were not oriented with respect to consistent global axes across accelerometers. Input stimuli were rectangular impulses, which were lowpass filtered (passband: $600\,\mathrm{Hz}$) to satisfy the Nyquist sampling criterion. The full width at half maximum of the impulse input was $1\,\mathrm{ms}$, and the average peak input acceleration at the actuator probe tip was $22.9\,\mathrm{m/s^2}$ across contact conditions. The measured skin accelerations were averaged across 8 trials and demeaned to produce the impulse responses, which were $400\,\mathrm{ms}$ in duration. Input stimuli were measured at the actuator probe tip for P1 and averaged across 7 trials. These input signals are provided with the toolbox to enable compensation of the actuator response in the impulse response measurements if desired. Data collection took approximately 2 hours per participant.

IV. Evaluating SkinSource Predictions

SkinSource employs the impulse response dataset and computational methods described in the prior sections to predict skin vibrations evoked in the upper limb for the conditions and input forces specified by the user. To evaluate the accuracy of this methodology, we compared SkinSource

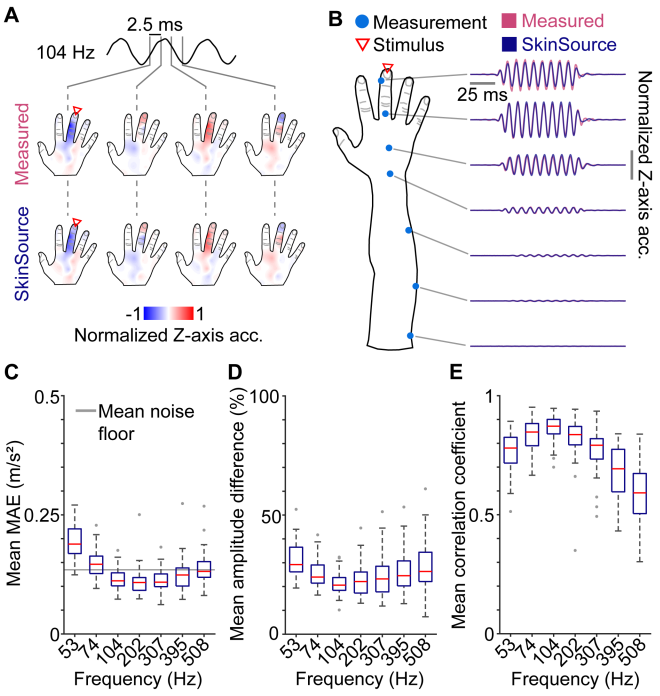

Fig. 4. **Comparison of measurements and SkinSource predictions.** A) Normalized z-axis skin accelerations from measurements (top) and SkinSource predictions (bottom) at consecutive time steps for a 104 Hz sinusoid applied at the tip of digit III (perpendicular) of Participant 1 (P1). Top trace shows the measured z-axis skin acceleration at the measurement location closest to the input location. B) Normalized z-axis skin accelerations at selected points (left, blue dots) on the upper limb of P1 from measurements (pink) and SkinSource predictions (dark blue) for a 104 Hz sinusoid applied at the tip of digit III (perpendicular). C) Mean MAE (mean absolute error), D) mean percent amplitude difference, and E) mean Pearson correlation coefficient between measurements and SkinSource predictions across input sinusoid frequency. In C-E, the mean is taken across all measurement locations and axes, then summarized as box plots across all participants and input locations for each frequency. Box limits: lower and upper quartiles; red center lines: median; whiskers: 1.5x interquartile range; gray dots: outliers.

predictions to experimental measurements of skin vibrations elicited by sinusoidal inputs (7 sinusoids spaced on a logarithmic scale from 53 to 508 Hz, 10 cycles, averaged across 5 trials). The experimental measurement procedure was identical to that used to measure the impulse responses (Section III). We computed the SkinSource predictions (Eq. 1) and assessed their similarity to the experimental measurements (Fig. 4A, B). To compare results across these two conditions, data was normalized by the average RMS signal amplitude within each condition. Skin vibrations were only compared at locations where the vibration amplitudes were at least twice the average measurement noise floor.

We analyzed errors averaged across measurement locations and axes for all participants and input frequencies. The errors quantified phase and amplitude differences between the SkinSource predictions and the measurements. The mean absolute error (MAE), which captured both phase and amplitude differences, was comparable to the average noise floor of the measurements (Fig. 4C). The median percent amplitude differences, which captured only amplitude errors, remained below 30 % across all frequencies (Fig. 4D). Additionally, median Pearson correlation coefficients, which captured only phase differences, were above 0.5 across all frequencies (Fig. 4E). Though correlations decreased at higher frequencies, which also led to an increase in MAE, prior work suggests that this may have little effect on perception [36]. Overall, the SkinSource predictions were in qualitative and quantitative agreement with the measurements. The small discrepancies between the two conditions may be due to differences in contact conditions, signal-to-noise ratio (SNR), or time alignment. Notably, measurement collection took approximately 2 hours per participant, while the SkinSource predictions were obtained in less than 5 s, highlighting the utility of SkinSource's data-driven methodology.

V. Linearity of Vibration Transmission in the Upper Limb

SkinSource leverages impulse responses that encode the physics of vibration transmission in the upper limb and enable the computational experiments described in this work. This approach relies upon the linearity of vibration transmission in the skin. Prior work has established the validity of this assumption within a stimulated digit [37]. Here, we confirm that vibration transmission across the entire upper limb behaves linearly over a wide range of input velocities, including those at which the SkinSource impulse response dataset was collected. To perform this validation, we conducted two experiments evaluating linearity via amplitude scaling (Linearity Experiment 1) and superposition (Linearity Experiment 2).

A. Experimental Setup

Skin velocities were measured at selected locations on the right hands and arms of two participants (P1 and P2; Fig. 5A) using a laser Doppler vibrometer (LDV; model PDV-100, Polytec, Irvine, CA; 48 kHz sample rate) placed normal to the skin at a distance of 30 cm above the participants' hands and arms. To ensure high SNR, small squares of adhesive retro-reflective tape (5 mm^2 area) were placed on the participants' skin at the measurement locations. The experimental setup was otherwise identical to that described in Section III.

B. Linearity Experiment 1: Amplitude Scaling

To test amplitude scaling, sinusoids (10 frequencies between 25 and 600 Hz) and a linear sine sweep (25 to 600 Hz; 5 s duration) were applied to the tip of digit III at 5 amplitude levels (5, 10, 20, 40, and 80 mm/s zero-to-peak loaded actuator velocities). Each input was repeated for 5 trials, and a compensation filter was applied to ensure that the actuator response was flat in frequency (within 10 % of the target velocity). In the SkinSource impulse response dataset, the maximum input velocity across all contact conditions was 21.6 mm/s.

After normalizing the sinusoid measurements by the input velocity, the responses of the lowest four amplitude levels were nearly indistinguishable (Fig. 5B, overlapped black traces). At the highest amplitude level (80 mm/s), nonlinearities became noticeable below 200 Hz and became more pronounced with increasing distance from the actuator

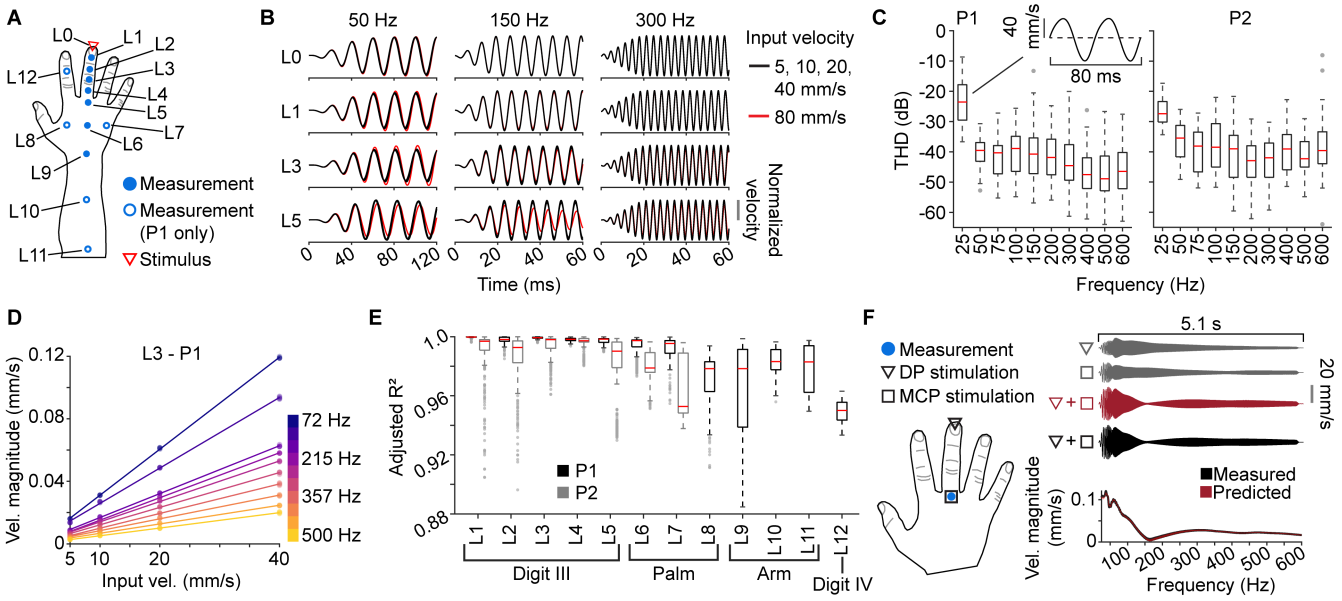

Fig. 5. **Validation of the linearity of vibration transmission in the upper limb.** A) Skin velocity was measured via laser Doppler vibrometry at selected locations (blue dots, L0-L12) on the dorsal surface of the hands of two participants (P1 and P2) during stimulation on the volar side of the distal phalanx of digit III (red arrow). L0 denotes the measurement location on the actuator probe tip. B) Measured velocity normalized by input velocity at 4 locations (L0, L1, L3, and L5) and 3 frequencies (50, 150, and 300 Hz), with measurements at all input velocities overlaid. Red trace corresponds to highest input velocity (80 mm/s). C) Boxplot of total harmonic distortion (THD) for the set of sinusoidal input signals, aggregated across all measured locations for each stimulus frequency. Shown for P1 (left) and P2 (right). Inset shows unloaded actuator response at 25 Hz. Box limits: lower and upper quartiles; red center lines: median; whiskers: 1.5x interquartile range; gray dots: outliers. D) Linear fits (lines) of input velocity versus measured velocity magnitude for all trials of sine sweep measurements (dots). Shown for P1 at L3 for selected frequency bins (denoted by color). E) Boxplots of adjusted R^2 from linear fits of sine sweep measurement frequency spectra (25-600 Hz for P1, 25-500 Hz for P2, 2 Hz resolution) aggregated across all trials and frequency bins for each measurement location (L1-L12). Box color: participant (P1: black, P2: gray); box limits: lower and upper quartiles; red center lines: median; whiskers: 1.5x interquartile range; gray dots: outliers. F) Predicted (red) versus measured (black) skin velocity at a selected location (blue dot) in the time and frequency domains during simultaneous DP (triangle) and MCP (square) stimulation. Predicted skin velocity is computed as the sum of measurements during DP-only and MCP-only stimulation (top, gray).

(Fig. 5B, red trace). We found evidence of modest shifts (approximately 25°) of the fundamental and large contributions of third-order harmonics, the latter of which is consistent with observations in brain tissue [38]. Due to the observed nonlinearities, we restricted further analysis to the lowest four amplitude levels ($\leq 40\,\mathrm{mm/s}$). We also found that the average total harmonic distortion (THD) of the sinusoid responses across all measured locations was $-40\,\mathrm{dB}$ (Fig. 5C). The increased THD at 25 Hz was primarily due to displacement limitations of the actuator (Fig. 5C, inset). The outliers present for P2 at 600 Hz were due to a large compensation factor that degraded actuator performance. For this reason, subsequent analyses for P2 were performed only up to 500 Hz.

We used the sine sweep measurements to analyze linearity across the entire frequency spectrum (25 to 600 Hz for P1, 25 to 500 Hz for P2, 2 Hz resolution). For each repetition and measured location, we computed the frequency spectrum of the skin vibrations and performed a linear regression on the spectrum amplitudes (Fig. 5D). The quality of the linear fit was assessed using the adjusted coefficient of determination (adjusted R^2), with a high adjusted R^2 indicating linearity. Amplitude levels that fell within $10\,\%$ of the average noise floor or that lacked consistent estimates across trials (index of dispersion > 0.02) were removed. The mean linear fit across the frequency spectra was nearly 1 at all locations (mean adjusted $R^2 = 0.99$; Fig. 5E). We found variations in the distributions of fits as we moved beyond digit III, likely due to lower SNR and spurious arm movements resulting in the deviation of the laser off of the reflective tape at the measurement locations.

C. Linearity Experiment 2: Superposition

Stimuli were applied in three contact conditions: at the distal phalanx (DP) of digit III (Condition 1), at the metacarpophalangeal joint (MCP) of digit III (Condition 2), and at the DP and MCP of digit III simultaneously (Condition 3; Fig. 5F, left). Stimuli were applied at only a single amplitude level (20 mm/s zero-to-peak loaded actuator velocity).

To confirm that vibrotactile transmission in the upper limb followed the superposition principle, we compared the measured vibrations during Condition 3 to the sum of independent measurements made during Conditions 1 and 2. Even in cases where significant destructive interference occurred at the measured location, the simultaneous application of sine sweeps at two locations (Condition 3) was nearly identical to the sum of skin vibrations elicited by sine sweeps applied at the two locations independently (Condition 1 + Condition 2; Fig. 5F, right). Across all locations for both participants, both the mean time-domain and frequency-domain Pearson correlation coefficients between Condition 1 + Condition 2 and Condition 3 were greater than 0.99, indicating that the superposition principle held.

D. Discussion

The SkinSource predictions (Eq. 1) rely on the principles of both amplitude scaling and superposition (i.e., linearity) to compute skin vibrations in the upper limb in response to arbitrary input forces applied at multiple input locations. The results of both experiments in this section indicate that the vibration transmission in the upper limb is linear at or below $40\,\mathrm{mm/s}$ (zero-to-peak), though the upper bound of this range may depend on actuator dynamics. Thus, for the ranges at which the SkinSource dataset was captured (maximum $21.6\,\mathrm{mm/s}$ peak velocity), impulse responses can be used to entirely characterize the upper limb vibration response.

VI. Conclusion

SkinSource provides data-driven upper limb models that allow users to predict the skin's vibration response to specified time-varying input forces supplied to numerous locations across the hand. In evaluations, we found that the SkinSource predictions accurately matched measurements of skin vibrations elicited under similar experimental conditions. Further, we confirmed that the entire upper limb can be considered as a linear medium for vibration transmission for input velocities within the range employed in SkinSource ($< 40\,\mathrm{mm/s}$ zero-to-peak). These results are generally consistent with prior literature on linearity within a stimulated digit [37]. The toolbox and dataset contributed by SkinSource provide a versatile framework for supporting haptics research at the intersection of mechanics, perception, and neuroscience. By reducing the need for time-intensive measurements using a data-driven computational methodology, SkinSource may aid in modeling vibrotactile transmission in the upper limb, understanding the neuromechanical basis of touch perception, and accelerating the design and engineering of novel haptic technologies.

Similar data-driven modeling techniques can be found in the field of audio engineering. These approaches involve encoding sound transfer from points in 3D space to the human ear, analogous to encoding vibration transmission in the skin. Measurements over large numbers of participants have enabled the personalization of 3D audio rendering based on user-specific anthropometric features, which has significantly improved the quality and accessibility of 3D audio reproduction over headphones [39]–[41]. Though SkinSource currently integrates only four upper limb models, which limits its ability to generalize across a more diverse population, the data-driven modeling techniques employed here may enable similar personalization for haptic rendering given larger datasets.

In its current form, SkinSource nevertheless provides a versatile computational testbed enabling the systematic study of vibration transmission in the hand and arm for applications in haptic research and design. However, our characterization of vibration transmission in the upper limb is not exhaustive and does not capture skin vibrations for all possible contact conditions, upper limbs, input locations, or output locations. Notably, the spatial resolution of SkinSource output locations does not satisfy the spatial Nyquist sampling criterion, which requires that high-frequency skin vibrations ($\geq 300\,\mathrm{Hz}$) be sampled at $\leq 1\,\mathrm{cm}$ spacing to accurately predict vibrations at points between measurement locations [8]. In addition, to mitigate low-frequency artifacts and satisfy the temporal Nyquist sampling criterion at high frequencies, SkinSource input signals should be bandlimited between 25 and $600\,\mathrm{Hz}$. This frequency range nonetheless encompasses a large proportion of frequencies relevant to vibrotactile perception, particularly for Pacinian and Meissner corpuscle mechanoreceptors [42]. Finally, SkinSource predicts skin vibrations in response to stimuli applied normally to the skin surface using a contact surface with dimensions of $7\times7\,\mathrm{mm}$. Some differences in the amplitude and phase of the upper limb skin response would be expected for stimuli applied in shear directions or with different contact conditions. These constraints highlight several opportunities for extending this work in the future.

Acknowledgement

This work was supported by a Link Foundation Modeling, Simulation, and Training Fellowship and UC Santa Barbara Graduate Opportunity Fellowship to N.T, the Italian Ministry of Education and Research (MIUR) in the framework of the FoReLab project (Departments of Excellence) to S.F. and M.B, and National Science Foundation awards No. 2139319 to D.G and No. 1751348 to Y.V. We thank Yitian Shao for assistance with data collection and Hannes Saal for valuable feedback.

References

[1] Benoit Delhaye, Vincent Hayward, Philippe Lefevre, and Jean-Louis Thonnard. Texture-induced vibrations in the forearm during tactile exploration. *Frontiers in Behavioral Neuroscience*, 2012.

[2] Yitian Shao, Vincent Hayward, and Yon Visell. Spatial patterns of cutaneous vibration during whole-hand haptic interactions. *Proceedings of the National Academy of Sciences*, 2016.

[3] Xavier Libouton, Olivier Barbier, Yorick Berger, Leon Plaghki, and Jean-Louis Thonnard. Tactile roughness discrimination of the finger pad relies primarily on the vibration sensitive afferents not necessarily located in the hand. *Behavioural Brain Research*, 2012.

[4] Louise R. Manfredi, Hannes P. Saal, Kyler J. Brown, Mark C. Zielinski, John F. Dammann, Vicky S. Polashock, and Sliman J. Bensmaia. Natural scenes in tactile texture. *Journal of Neurophysiology*, 2014.

[5] Yitian Shao, Vincent Hayward, and Yon Visell. Compression of dynamic tactile information in the human hand. *Science Advances*, 2020.

[6] T. J. Moore. A survey of the mechanical characteristics of skin and tissue in response to vibratory stimulation. *IEEE Transactions on Man-Machine Systems*, 1970.

[7] Benjamin H. Pubols. Effect of mechanical stimulus spread across glabrous skin of raccoon and squirrel monkey hand on tactile primary afferent fiber discharge. *Somatosensory Research*, 1987.

[8] Louise R. Manfredi, Andrew T. Baker, Damian O. Elias, John F. Dammann Iii, Mark C. Zielinski, Vicky S. Polashock, and Sliman J. Bensmaia. The effect of surface wave propagation on neural responses to vibration in primate glabrous skin. *PLOS ONE*, 2012.

[9] Hannes P. Saal, Benoit P. Delhaye, Brandon C. Rayhaun, and Sliman J. Bensmaia. Simulating tactile signals from the whole hand with millisecond precision. *Proceedings of the National Academy of Sciences*, 2017.

[10] J. W. Andrews, M. J. Adams, and T. D. Montenegro-Johnson. A universal scaling law of mammalian touch. *Science Advances*, 2020.

[11] Davide Deflorio, Massimiliano Di Luca, and Alan M. Wing. Skin and mechanoreceptor contribution to tactile input for perception: A review of simulation models. *Frontiers in Human Neuroscience*, 2022.

[12] Udaya B. Rongala, Andre Seyfarth, Vincent Hayward, and Henrik Jörntell. The import of skin tissue dynamics in tactile sensing. *bioRxiv*, 2023.

[13] Neeli Tummala, Yitian Shao, and Yon Visell. Spatiotemporal organization of touch information in tactile neuron population responses. In *2023 IEEE World Haptics Conference*, 2023.

[14] Bharat Dandu, Yitian Shao, and Yon Visell. Rendering spatiotemporal haptic effects via the physics of waves in the skin. *IEEE Transactions on Haptics*, 2020.

[15] Valerie de Vlam, Michaël Wiertlewski, and Yasemin Vardar. Focused vibrotactile stimuli from a wearable sparse array of actuators. *IEEE Transactions on Haptics*, 2023.

[16] Ravi Balasubramanian and Veronica J. Santos, editors. *The Human Hand as an Inspiration for Robot Hand Development*, volume 95 of *Springer Tracts in Advanced Robotics*. Springer Cham, 2014.

[17] Simone Fani, Katia Di Blasio, Matteo Bianchi, Manuel Giuseppe Catalano, Giorgio Grioli, and Antonio Bicchi. Relaying the high-frequency contents of tactile feedback to robotic prosthesis users: Design, filtering, implementation, and validation. *IEEE Robotics and Automation Letters*, 2019.

[18] Luyao Wang, Lihua Ma, Jiajia Yang, and Jinglong Wu. Human somatosensory processing and artificial somatosensation. *Cyborg and Bionic Systems*, 2021.

[19] Takayuki Iwamoto and Hiroyuki Shinoda. Finger ring tactile interface based on propagating elastic waves on human fingers. In *Second Joint EuroHaptics Conference and Symposium on Haptic Interfaces for Virtual Environment and Teleoperator Systems (WHC'07)*, 2007.

[20] Chris Harrison, Desney Tan, and Dan Morris. Skinput: appropriating the body as an input surface. In *Proceedings of the SIGCHI Conference on Human Factors in Computing Systems*, 2010.

[21] Taku Hachisu, Gregory Reardon, Yitian Shao, Kenji Suzuki, and Yon Visell. Interpersonal vibrotactile feedback via waves transmitted through the skin: Mechanics and perception. In *2020 IEEE Haptics Symposium*, 2020.

[22] Yitian Shao, Hui Hu, and Yon Visell. A wearable tactile sensor array for large area remote vibration sensing in the hand. *IEEE Sensors Journal*, 2020.

[23] Stejara Dinulescu, Neeli Tummala, Gregory Reardon, Bharat Dandu, Dustin Goetz, Sven Topp, and Yon Visell. A smart bracelet supporting tactile communication and interaction. In *2022 IEEE Haptics Symposium*, 2022.

[24] Ren G. Dong, John Z. Wu, Xueyan S. Xu, Daniel E. Welcome, and Kristine Krajnak. A review of hand–arm vibration studies conducted by us niosh since 2000. *Vibration*, 2021.

[25] Steven P. Kearney, Altaf Khan, Zoujun Dai, and Thomas J. Royston. Dynamic viscoelastic models of human skin using optical elastography. *Physics in Medicine Biology*, 2015.

[26] Michael Wiertlewski and Vincent Hayward. Mechanical behavior of the fingertip in the range of frequencies and displacements relevant to touch. *Journal of Biomechanics*, 2012.

[27] Gregory Reardon, Bharat Dandu, Yitian Shao, and Yon Visell. Shear shock waves mediate haptic holography via focused ultrasound. *Science Advances*, 2023.

[28] Giulia Corniani, Zing S Lee, Matt J Carré, Roger Lewis, Benoit P Delhaye, and Hannes P Saal. Sub-surface deformation of individual fingerprint ridges during tactile interactions. *bioRxiv*, 2023.

[29] Aram Z Hajian and Robert D Howe. Identification of the mechanical impedance at the human finger tip. *Journal of Biomechanical Engineering*, 1997.

[30] Toshio Tsuji, Pietro G Morasso, Kazuhiro Goto, and Koji Ito. Human hand impedance characteristics during maintained posture. *Biological Cybernetics*, 1995.

[31] Heather Culbertson, Juan José López Delgado, and Katherine J. Kuchenbecker. One hundred data-driven haptic texture models and open-source methods for rendering on 3d objects. In *2014 IEEE Haptics Symposium*, 2014.

[32] Katherine O. Sofia and Lynette A. Jones. Mechanical and psychophysical studies of surface wave propagation during vibrotactile stimulation. *IEEE Transactions on Haptics*, 2013.

[33] Valay A. Shah, Maura Casadio, Robert A. Scheidt, and Leigh A. Mrotek. Vibration propagation on the skin of the arm. *Applied Sciences*, 2019.

[34] Alexis Devillard, Aruna Ramasamy, Damien Faux, Vincent Hayward, and Etienne Burdet. Concurrent haptic, audio, and visual data set during bare finger interaction with textured surfaces. In *2023 IEEE World Haptics Conference*, 2023.

[35] Velko Vechev, Juan Zarate, David Lindlbauer, Ronan Hinchet, Herbert Shea, and Otmar Hilliges. Tactiles: Dual-mode low-power electromagnetic actuators for rendering continuous contact and spatial haptic patterns in vr. In *2019 IEEE Conference on Virtual Reality and 3D User Interfaces*, 2019.

[36] Sliman J. Bensmaıa and Mark Hollins. Complex tactile waveform discrimination. *The Journal of the Acoustical Society of America*, 2000.

[37] Camille Fradet, Louise R. Manfredi, Sliman Bensmaia, and Vincent Hayward. Fingertip skin as a linear medium for wave propagation. In *2017 IEEE World Haptics Conference*, 2017.

[38] KK Darvish and JR Crandall. Nonlinear viscoelastic effects in oscillatory shear deformation of brain tissue. *Medical Engineering & Physics*, 2001.

[39] Henrik Møller, Michael Friis Sørensen, Clemen Boje Jensen, and Dorte Hammershøi. Binaural technique: Do we need individual recordings? *Journal of the Audio Engineering Society*, 1996.

[40] Kazuhiro Iida, Yohji Ishii, and Shinsuke Nishioka. Personalization of head-related transfer functions in the median plane based on the anthropometry of the listener's pinnae. *The Journal of the Acoustical Society of America*, 2014.

[41] Edgar A Torres-Gallegos, Felipe Orduna-Bustamante, and Fernando Arámbula-Cosío. Personalization of head-related transfer functions (hrtf) based on automatic photo-anthropometry and inference from a database. *Applied Acoustics*, 2015.

[42] R. S. Johansson, U. Landström, and R. Lundström. Responses of mechanoreceptive afferent units in the glabrous skin of the human hand to sinusoidal skin displacements. *Brain Research*, 1982.